Theoretical study on the correlation between open-shell electronic structures and third-order nonlinear optical properties in one-dimensional chains of π-radicals

Jinki Shoda[a], Masako Yokoyama[a], Wataru Yoshida[a], Hiroshi Matsui[b], Ryota Sugimori[a], Ryohei Kishi [a,c,d,e], Yasutaka Kitagawa[a,c,d,e,f]*

[a] Department of Materials Engineering Science, Graduate School of Engineering Science, Osaka University, Toyonaka, Osaka 560-8531, Japan

[b] Osaka Institute of Public Health, 1-3-3 Nakamichi, Higashinari-ku, Osaka 537-0025, Japan

[c] Center for Quantum Information and Quantum Biology Division (QIQB), Osaka University, Toyonaka, Osaka 560-8531, Japan

[d] Research Center for Solar Energy Chemistry (RCSEC), Graduate School of Engineering Science, Osaka University, Toyonaka, Osaka 560-8531, Japan

[e] Innovative Catalysis Science Division, Institute for Open and Transdisciplinary Research Initiatives (ICS-OTRI), Osaka University, Suita, Osaka 565-0871, Japan

[f] Spintronics Research Network Division, Institute for Open and Transdisciplinary Research Initiatives (OTRI-Spin), Osaka University, Toyonaka, Osaka 560-8531, Japan

ABSTRACT

This paper theoretically investigated the correlation between open-shell electronic structure and third-order nonlinear optical (NLO) properties of one-dimensional (1D) stacked chains of π-radicals. By employing the finite *N*-mer models consisting of methyl or phenalenyl radicals with different stacking distances, we evaluated the average and standard deviation of diradical characters y_i for *N*-mer models of π-radicals (y_{av} and y_{SD}). Then, we estimated these diradical characters at the limit $N \rightarrow \infty$. These *y*-based indices were helpful in discussing the correlation between the open-shell electronic structures and the second hyperpolarizability per dimer at the limit $N \rightarrow \infty$, γ_∞, for the 1D chains with stacking distance alternation (SDA). The calculated γ_∞ values and the polymer/dimer ratio $\gamma_\infty/\gamma(N = 2)$ were enhanced significantly when both the stacking distance and the SDA are small. We also found that the spin-unrestricted long-range corrected (LC-)UBLYP method with the range-separating parameter $\mu = 0.47$ bohr^{-1} reproduced well the trend of γ_∞ of this type of 1D chains estimated at the spin-unrestricted coupled-cluster levels. The present study is expected to contribute to establishing the design guidelines for future high-performance open-shell molecular NLO materials.

1. INTRODUCTION

For the past two decades, molecular materials exhibiting large third-order nonlinear optical (NLO) responses have been actively explored because such materials are essential for establishing future photonic and optoelectronic devices[1]. Molecular third-order NLO materials have advantages in their fast response time and molecular design feasibility compared with inorganic crystals. Numerous theoretical and experimental studies have been carried out to clarify design guidelines for molecular third-order NLO materials[2–8]. In addition to the molecular materials based on the stable closed-shell molecules, open-shell systems[9–14], such as diradicals, multiradical systems, and high-spin species, have recently been focused on as candidates for novel third-order NLO materials. Nakano et al. theoretically clarified the relationship between the diradical character *y* (a theoretical index characterizing the degree of open-shell in the singlet state) and the molecular second hyperpolarizability γ (the third-order NLO property at the molecular scale)[13]. They found that singlet diradicals and diradical-like molecules with intermediate *y* exhibit enhanced γ compared to closed-shell and complete open-shell counterparts. Recent advances in synthesis and measurement techniques have contributed to establishing open-shell third-order NLO materials [15–19].

The (partially) unpaired electrons in the open-shell molecules are sensitive to external stimuli, leading to their significant NLO property and high chemical reactivity. These highly active unpaired electrons often contribute to σ-bond formation with other open-shell molecules, which results in reducing their high response properties. Therefore, practical design strategies are needed to suppress the formation of σ-bonds while maintaining the activity and sensitivity of the unpaired electrons. In such situations, these unpaired electrons can be utilized to achieve huge response properties in their molecular assembly that cannot be achieved with single molecules alone. Several π-dimers exhibiting open-shell electronic structures have been realized by tuning the balance between the attractive and repulsive interactions between the open-shell π-conjugated molecules[20]. Notably, derivatives of phenalenyl radicals[21–23] and cyclic thiazyl radicals[24–27], typical neutral π-radicals with high thermodynamic stabilities, were reported to form one-dimensional (1D) π-stacked chains in the crystalline phase, in which each monomer interacts with each other via the pancake bonding interaction[28–32]. Their stacking distances and relative configurations can be controlled by chemical modifications while maintaining the high activity of the unpaired electrons [28–32].

Several theoretical and computational studies have evaluated the third-order NLO properties of such 1D chains of monoradicals. Nakano et al. employed the simplest 1D chain model of hydrogen atoms and averaged y (y_{av}) values to characterize their open-shell characters[33]. They found that γ per unit in the 1D chains (multiradical) takes a maximum in a smaller y_{av} region compared with the diradical systems. Yoneda et al. performed the density functional theory (DFT) calculations for π-dimers of phenalenyl radicals with different stacking distances d in the singlet state [29]. They found that y of the dimer decreases as decreasing d, and γ per monomer takes the maximum around d = 2.9 Å, at which y is in the intermediate region. Salustro et al. evaluated the γ_∞ of 1D chains of phenalenyl radicals[32] by extending the coupled-perturbed Kohn-Sham (CPKS) analytic derivative method under the periodic boundary condition implemented in the CRYSTAL package[34,35], which was the first direct computation of γ_∞ of this type of 1D chain. In a series of theoretical studies, Matsui et al. investigated the effects of increasing the number of monomers (N) on the γ per unit based on the 1D chains of hydrogens and cyclic thiazyl radicals[31]. They estimated the γ per unit in the limit $N \rightarrow \infty$ (γ_∞) by extrapolating the results of N-mers. These studies predicted that the third-order NLO properties of closely stacked 1D chains of π-radicals are comparable to those of π-conjugated polymers, suggesting through-space (TS) conjugation in such systems.

We expect that y_{av} can fairly characterize the degree of open-shell in the 1D chains of π-radicals with the uniform stacking distance d. Of course, realizing 1D chains of π-radicals with a uniform stacking distance is challenging. Even if 1D chains are formed successfully in crystalline, alternations of the stacking distance often appear. In such a situation, y_{av} may not always uniquely characterize their open-shell electronic structures related to the third-order NLO responses. Here, we considered introducing another y-based index, y_{SD}, corresponding to the standard deviation of y, and examined how y_{av} and y_{SD} can help characterize the open-shell electronic structure of the stacked 1D chains of π-radicals where two types of stacking distance, d_1 and d_2, appear alternately. Then, we investigated the dependence of stacking distance alternation (SDA) on y_{av} , y_{SD}, and γ_∞ in 1D chain models of π-radicals based on quantum chemical calculations.

2. CALCULATED MODELS AND CALCULATION METHODS

2.1 Average and standard deviation of diradical characters

This section briefly explains how y_{av} and y_{SD} characterize the open-shell electronic structures of the 1D chains. **Figures 1a** and **1b** show the models of 1D chains composed of methyl and phenalenyl radicals. We employed the sp^2 methyl radical[36] and the phenalenyl radical as a monomer unit. **Figure 1c** illustrates their dimer's frontier orbital energy levels (N = 2) and tetramers (N = 4). It is known that there is a good negative correlation between y and the energy gap between the highest occupied and lowest unoccupied molecular orbitals (HOMO and LUMO) for diradicaloids. The HOMO and LUMO are constructed by bonding and anti-bonding interactions of the singly occupied MOs (SOMOs) of the monomers. Thus, the HOMO-LUMO gap of the dimer tends to increase with decreasing the stacking distance d_1 in the dimer unit.

For the multiradicaloids ($N \geq 4$), we can define plural diradical characters y_i from the occupation numbers of the i-th pair of natural orbitals (NOs), i.e., HONO-i and LUNO+i. Roughly, y_i (i = 0, 1, … N/2–1) is negatively correlated with the energy gap between the HOMO-i and LUMO+i. When the tetramer is composed of two almost non-interacting dimers with $d_2 >> d_1$, the orbital interaction between the HOMOs (LUMOs) of the dimer can be negligible. As a result, the HOMO and HOMO-1 (LUMO and LUMO+1) of the tetramer with $d_2 >> d_1$ are nearly degenerated. Thus, we will obtain $y_0 \sim y_1$ in such a situation. When $d_2 \sim d_1$ (and they are sufficiently small), the orbital interaction between the HOMOs (LUMOs) of the dimer becomes considerable, resulting in $y_0 >> y_1$. Since we define y_{av} by the arithmetic average of $\{y_i\}$, we can find situations where y_0 and y_1 are different but y_{av} is similar. Thus, in addition to y_{av}, we here introduce another y-based index, the standard deviation of y_i, denoted as y_{SD}. We can expect that, for example, $y_{SD} \sim 0$ for the non-interacting dimers, but $y_{SD} > 0$ for the interacting dimers. For $N \rightarrow \infty$, if the conduction and valence bands are constructed primarily from the SOMOs of the monomers, we can consider these indices at $N \rightarrow \infty$, i.e., $y_{av}(N \rightarrow \infty)$ and $y_{SD}(N \rightarrow \infty)$. These indices are related to the averaged band gap and widths. Generally, the band gap and widths are essential for characterizing the optical response properties.

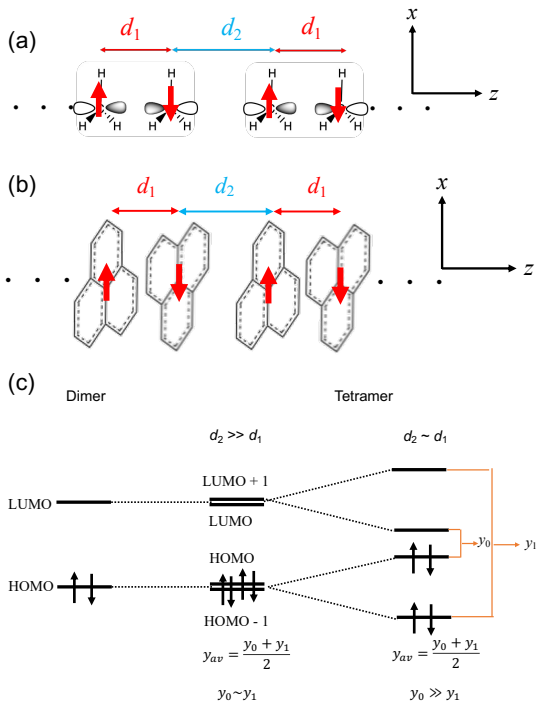

Figure 1. Structures of 1D chain models consisting of (a) methyl radicals, and (b) phenalenyl radicals, and (c) orbital interaction diagram for the tetramers with different staking distance alternations.

2.2 Computational details

We employed the molecular geometry of methyl radical optimized at the UCCSD(T)/aug-cc-pVDZ level under the D_{3h} symmetry constraint[36]. Then, eclipsed-stacking 1D N-mer models [$(CH_3)_N$] were constructed, keeping the intramolecular geometries fixed.

The y_i values for the N-mer were calculated at the projected unrestricted Hartree-Fock (PUHF) level using Yamaguchi's equation [eq. (1)][37],

$$y_i = 1 - \frac{2T_i}{1 + T_i^2} \qquad (1)$$

Here T_i is calculated from the occupation numbers n of NOs at the UHF level

$$T_i = \frac{n_{\mathrm{HONO}-i} - n_{\mathrm{LUNO}+i}}{2} \tag{2}$$

The y_{av} for the N-mer is defined by the following equation.

$$y_{\mathrm{av}}(N) = \sum_{i=0}^{N/2-1} y_i(N) \tag{3}$$

Note that there are $N/2$ radical pairs in the N-mer. Then, the standard deviation y_{SD} is defined by the following equation.

$$y_{\mathrm{SD}}(N) = \sqrt{\frac{1}{N/2}\sum_{i=0}^{N/2-1} (y_i(N) - y_{\mathrm{av}}(N))^2} \tag{4}$$

For $N = 4$, y_{av} and y_{SD} are expressed by the following equations,

$$y_{\mathrm{av}}(N = 4) = \frac{y_0 + y_1}{2} \tag{5}$$

$$y_{\mathrm{SD}}(N = 4) = \frac{y_0 - y_1}{2} \tag{6}$$

We then computed the stacking direction component of the static γ values of N-mer $\gamma(N) = \gamma_{zzzz}(N)$. The $\gamma(N)$ values were evaluated using the finite-field method. We employed the fourth-order

numerical derivative of total energy under the static electric field in the range from 5.0 x 10^{-4} a.u to 6.0 x 10^{-3} a.u., which gives the relative errors of about 1% for γ.

The total energies in the presence of an electric field were evaluated at the spin-unrestricted coupled-cluster singles and doubles with triples corrections [UCCSD(T)] and the long-range corrected (LC-)UBLYP[38,39] levels. Previous studies usually evaluated the γ values at the LC-UBLYP level with μ = 0.33 $bohr^{-1}$. This range-separating parameter μ is known to reproduce the results based on the highly correlated UCCSD(T) for several intramolecular diradicaloids and dimers of π-radicals[40]. In this study, we compared the calculation results of LC-UBLYP using μ = 0.33 $bohr^{-1}$ and 0.47 $bohr^{-1}$ with the UCCSD(T) results for *N*-mers. During the calculations, we prepared an initial guess for the singlet state with the all-antiparallel spin alignment. We employed the 6-31+G basis set used in the previous studies for 1D stacked systems consisting of a methyl radical model. All these calculations were conducted by Gaussian 09 rev. D.[41]

After that, we tried to estimate y_{av}, y_{SD}, and γ at the limit of $N \rightarrow \infty$. We fitted the calculation results of

$$\Delta\gamma(N) = \frac{\gamma(N+2) - \gamma(N)}{2} \tag{7}$$

with the form of

$$\Delta\gamma(N) = \gamma_{\infty} - b\exp(-cN) \tag{8}$$

and then estimated γ_{∞}.[31] We also fitted the results of $y_{av}(N)$ and $y_{SD}(N)$ with the same exponential form as eq.(8) to calculate these values at the limit of $N \rightarrow \infty$, $y_{av,\infty}$ and $y_{SD,\infty}$.

We also considered 1D stacked chains of phenalenyl radicals. Geometry optimization for the phenalenyl monomer was performed at the UB3LYP/6-31G* level. Then, we constructed π-stacked *N*-mer models $(PLY)_N$ in the anti-parallel configuration (see **Figure 1a**) to evaluate y_i of

the *N*-mers at the PUHF level. We directly computed γ_∞ of the infinite 1D chain at the LC-UBLYP(μ = 0.47 bohr^{-1})/6-31G* level using the CRYSTAL 17 package. Details of the DFT calculations under the periodic boundary condition for 1D chains of phenalenyl radicals are discussed in the later section.

3. RESULTS AND DISCUSSION

3.1 1D chains of methyl radicals

Figure 2 shows the stacking distance (d_1) dependences of y_0 and $\gamma(N = 2)$ for the methyl radical π-dimer calculated at the PUHF/6-31+G and UCCSD(T)/6-31+G levels, respectively. y_0 decreased monotonically with decreasing d_1. $\gamma(N = 2)$ showed a bell-shaped dependence on d_1 with a maximum [$\gamma(N = 2)$ = 31 x 10^3 a.u.] around d_1 = 2.8-2.9 Å where y is in the intermediate region (y_0 = 0.45 at d_1 = 2.8 Å, and y_0 = 0.51 at d_1 = 2.9 Å).

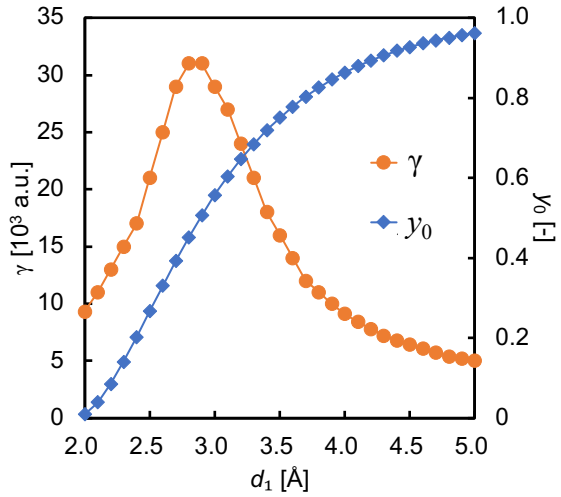

Figure 2. Stacking distance [d_1 (= d_2)] dependences of y_0 and static $\gamma(N = 2)$ for the methyl radical π-dimer calculated at the PUHF and UCCSD(T) levels, respectively, using the 6-31+G basis set.

We constructed 1D *N*-mer models of methyl radicals with different d_1 and d_2: **A1**(2.5 Å, 2.5 Å), **B1**(3.0 Å, 3.0 Å), **C1**(3.5 Å, 3.5 Å), **A2**(2.5 Å, 3.0 Å), **B2**(3.0 Å, 3.5 Å), and **C2**(3.5 Å, 4.0

Å). Note that, for the dimer, $y_0 = 0.27$ and $\gamma(N = 2) = 21 \times 10^3$ a.u. at $d_1 = 2.5$ Å, $y_0 = 0.56$ and $\gamma(N = 2) = 29 \times 10^3$ a.u. at $d_1 = 3.0$ Å, and $y_0 = 0.75$ and $\gamma(N = 2) = 16 \times 10^3$ a.u. at $d_1 = 3.5$ Å, respectively. **A1**-**C1** are the SDA-less ($d_2 = d_1$) models whereas **A2**-**C2** exhibit the SDA pattern with $d_2 = d_1 + 0.5$ Å. **Figure 3** shows the $y_{av}(N)$ and $y_{SD}(N)$ variations for these models with increasing N calculated at the PUHF/6-31+G level. The convergence behavior of $y_{SD}(N)$ is relatively slow compared to $y_{av}(N)$. **Table 1** shows the results of $y_{av,\infty}$ and $y_{SD,\infty}$ estimated by the fitting scheme. $y_{av,\infty}$ was almost determined by d_1. Namely, the $y_{av,\infty}$ values of **A*n*** were almost the same. On the other hand, $y_{SD,\infty}$ was in the order of **A1** > **B1** > (**A2**, **C1**, **B2**) > **C2**. From this result, $y_{SD,\infty}$ depends on the ratio d_2/d_1 as well as d_1 itself. **A1** and **A2** exhibited similar $y_{av,\infty}$ but different $y_{SD,\infty}$.

In **Figure 3c**, we plotted the convergence behaviors of $\Delta\gamma(N)$ with increasing N for these models. **A1** showed a slow convergence behavior of with N. **A2** also showed a relatively slow convergence behavior compared with other systems. These features reflected that the intermolecular interactions become significant when the stacking distances are small. **Table 1** also summarizes the results of γ_∞ and the ratio of γ_∞ from the γ of the dimer with the same d_1, i.e., $\gamma_\infty/\gamma(N = 2)$. The "polymer/dimer" ratio $\gamma_\infty/\gamma(N = 2)$ was in the order of **A1** > **A2** > **B1** > (**C1**, **B2**) > **C2**. From these results, the polymer/dimer ratio $\gamma_\infty/\gamma(N = 2)$ tends to be enhanced significantly when i) $y_{av,\infty}$ is in the small-medium region and then ii) $y_{SD,\infty}$ is large. The condition i) was already discussed in the previous paper[33]. For the condition ii), effect of the SDA ratio d_2/d_1 was usually discussed [33]. However, we can consider different situations affecting the tendency of $y_{SD,\infty}$, e.g., relative orientations of monomers in 1D chains. We will discuss this situation in the final section.

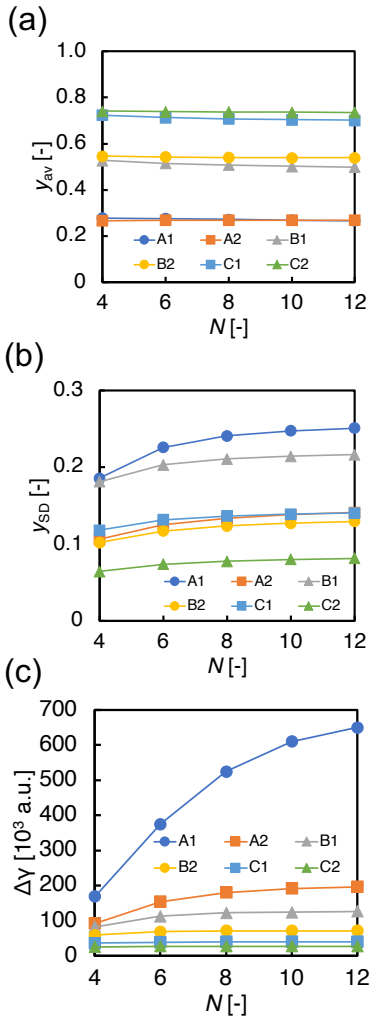

Figure 3. N dependence of (a) y_{av} and (b) y_{SD} calculated at the PUHF/6-31+G level, and (c) Δγ calculated at the UCCSD(T)/6-31+G level.

Table 1. Results of $y_{av\infty}$, $y_{SD,\infty}$ and γ_∞ were obtained by fitting the results in **Figure 3**.

Model (d_1, d_2)	$y_{av,\infty}$	$y_{SD,\infty}$	γ_∞ [10^3 a.u.]	$\gamma_\infty/\gamma(N=2)$ [-]
A1 (2.5Å, 2.5Å)	0.26	0.25	740	36.0
A2 (2.5Å, 3.0Å)	0.27	0.15	200	9.6
B1 (3.0Å, 3.0Å)	0.48	0.22	128	4.4
B2 (3.0Å, 3.5Å)	0.54	0.13	72	2.4

C1 (3.5Å, 3.5Å)	0.69	0.14	42	2.7
C2 (3.5Å, 4.0Å)	0.73	0.08	28	1.8

Next, we examined the exchange-correlation (xc-)functional dependence of γ_∞ when we employ the Kohn-Sham DFT method to calculate γ_∞. Indeed, applications of the UCCSD(T) method to the 1D chains of phenalenyl radicals and other realistic systems are usually infeasible. Among the xc-functionals, the LC-UBLYP with the range-separating parameter $\mu = 0.33$ bohr^{-1} [denoted as LC-UBLYP(0.33)] is known to reproduce well the γ values at the UCCSD(T) level for several diradical(oid)s with medium-large y.[40] However, it was also suggested that the LC-UBLYP(0.33) tends to overestimate the UCCSD(T) results for systems with small y, where γ_∞ is expected to increase significantly in the 1D chains (multiradicals). Thus, we conducted the LC-UBLYP calculations with different μ values (0.33 bohr^{-1} and 0.47 bohr^{-1}) for the 1D chain models of methyl radicals and compared the results with those of UCCSD(T).

In **Figure 4**, we compared the results of $\Delta\gamma(N)$ of **B1** calculated at the UCCSD(T), LC-UBLYP(0.47), and LC-UBLYP(0.33) levels with the 6-31+G basis set. In this model, the LC-UBLYP(0.33) overestimated the $\Delta\gamma(N)$ values of UCCSD(T) significantly for $N \geq 4$, although the result was close to the reference value for $N = 2$ [39.9 x 10^3 a.u. at the UCCSD(T), 35.3 x 10^3 a.u. at the LC-UBLYP(0.33), and 19.2 x 10^3 a.u. at the LC-UBLYP(0.47), respectively]. The LC-UBLYP(0.47) underestimated the $\Delta\gamma(N)$ values of UCCSD(T) to some extent, but their convergence behaviors look similar. Since the $\Delta\gamma(N)$ values and their convergence behaviors depend on the model, we summarized the results of γ_∞ and the polymer/dimer ratio $\gamma_\infty/\gamma(N = 2)$ for all the models in **Table 2**. The γ_∞ values and the polymer/dimer ratio $\gamma_\infty/\gamma(N = 2)$ at the LC-UBLYP(0.33) level were more than twice as large as those at the UCCSD(T) level for all these models. Overestimations of the LC-UBLYP(0.33) became especially significant when d_1 was small. On the other hand, the LC-UBLYP(0.47) results reproduced better the UCCSD(T) results for both the γ_∞ and $\gamma_\infty/\gamma(N = 2)$ compared with the LC-UBLYP(0.33).

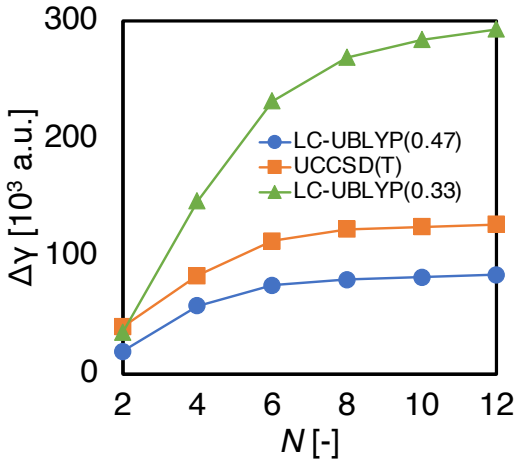

Figure 4. N dependence of $\Delta\gamma$ [10^3 a.u.] of **B1** calculated at the UCCSD(T), LC-UBLYP(0.33) and LC-UBLYP(0.47) levels with the 6-31+G basis set.

Table 2. Results of γ_∞ [10^3 a.u.] calculated at the UCCSD(T), LC-UBLYP(0.47) and LC-UBLYP(0.33) levels with the 6-31+G basis set. Values in round parenthesis are the polymer/dimer ratio $\gamma_\infty/\gamma(N=2)$ [-] where $\gamma(N=2)$ was calculated at d_1 at the same level of approximation.

Model (d_1, d_2)	UCCSD(T)	LC-UBLYP(0.33)	LC-UBLYP(0.47)
A1 (2.5Å, 2.5Å)	740 (36)	3200 (110)	550 (23)
A2 (2.5Å, 3.0Å)	200 (9.6)	590 (21)	180 (7.4)
B1 (3.0Å, 3.0Å)	130 (4.4)	300 (8.4)	84 (4.4)
B2 (3.0Å, 3.5Å)	72 (2.5)	140 (4.1)	49 (2.6)
C1 (3.5Å, 3.5Å)	42 (2.7)	84 (3.2)	30 (2.5)
C2 (3.5Å, 4.0Å)	28 (1.8)	55 (2.1)	22 (1.8)

We also performed the hyperpolarizability (γ-)density analysis[42] to examine the third-order electronic polarizations at these DFT levels. The γ-density, $\rho^{(3)}_{zzz}(\boldsymbol{r})$, is defined as the third-order field-induced response of charge density:

$$\rho_{zzz}^{(3)}(\boldsymbol{r}) = \left.\frac{\partial^3 \rho(\boldsymbol{r}, F_z)}{\partial F_z^3}\right|_{F_z=0} \quad (9)$$

where $\rho(\boldsymbol{r}, F_z)$ is the electron density at the position $\boldsymbol{r}$ in the presence of static electric field along the z-axis, F_z. $\rho_{zzz}^{(3)}(\boldsymbol{r})$ relates to γ_{zzzz} by the following spatial integration.

$$\gamma_{zzzz} = -\frac{1}{3!}\int z\rho_{zzz}^{(3)}(\boldsymbol{r})d\boldsymbol{r}^3 \quad (10)$$

Thus, the γ-density represents the spatial contributions of γ. Unfortunately, the electron density at the UCCSD(T) level is not available from the Gaussian program package, and we instead performed the γ-density analysis at the UCCSD level. In **Table S1**, we summarized the results of γ_∞ at the UCCSD/6-31+G level and the ratio γ_∞(UCCSD)/γ_∞(UCCSD(T)). The UCCSD (with the 6-31+G) underestimated the UCCSD(T) results when d_1 was small, and their results were close to the LC-UBLYP(0.47) ones.

Figure 5 shows the γ-density maps of **A2** with $N = 2$ and 4 calculated at the UCCSD, LC-UBLYP(0.33), and LC-UBLYP(0.47) (in **Figure S2**, we also plotted the results for $N = 12$). Yellow and blue surfaces represent the increase and decrease of electron density when the static electric field F_z is applied to the system toward the direction illustrated in **Figure 5**. Thus, a pair of positive (yellow) and negative (blue) γ-densities represents the field-induced third-order electronic polarization (dipole moment). When the direction of the dipole moment vector of the pair is the same as that of the external field F_z, it contributes positively to the total γ (see the relation between $\rho_{zzz}^{(3)}(\boldsymbol{r})$ and γ_{zzzz}). For $N = 2$, although the amplitudes of positive and negative γ-densities on the carbon atoms were slightly more prominent in the LC-UBLYP(0.33) result than the other methods, the differences in the γ-density maps were very slight. For $N = 4$, positive and negative γ-densities are distributed alternately on each monomer. Similar alternation patterns of γ-densities were observed in tetramers of phenalenyl radicals [29]. The direction of the field-induced dipole moment of the inner monomers is opposite to that of the outer monomers. Thus, the total γ

becomes significant when the amplitudes of γ-density on the inner monomers are reduced, the situation of which indicates the delocalization of electrons over the whole system. In the UCCSD and LC-UBLYP(0.47) results, the amplitudes of γ-density on the inner monomers were slightly reduced compared with those of the outer monomers. The reduction of γ-densities on the inner monomers were more apparent in the LC-UBLYP(0.33) result. These results indicated that the LC-UBLYP(0.33) overestimated the delocalization of electrons over the dimer pairs when the external field was applied. Thus, the optimal value of μ for the 1D chains of interacting π-radicals can be more significant than that for the dimers to suppress the over-delocalization.

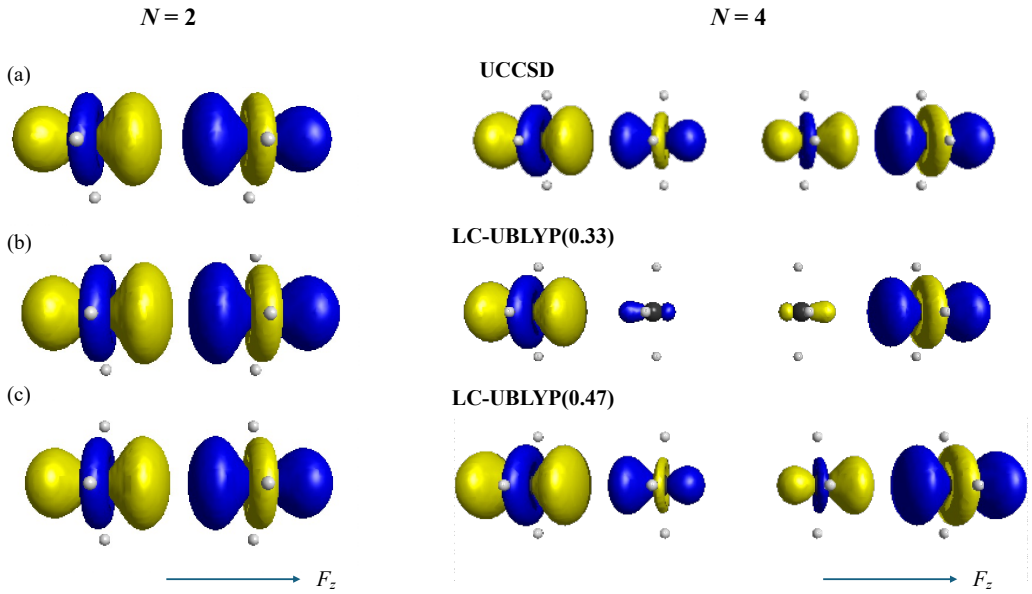

Figure 5. γ-density maps of **A2** (N = 2 and 4) at the (a) UCCSD, (b) LC-UBLYP(0.33), and (c) LC-UBLYP(0.47) levels. Yellow and blue surfaces represent the isosurfaces of $\rho^{(3)}_{zzz}(\boldsymbol{r})$ with the contour values of ± 100 a.u.

3.2 1D chains of phenalenyl radicals

We also investigated the open-shell characters and third-order NLO properties of 1D chains of phenalenyl radicals. First, we calculated y and γ(N = 2) as a function of d_1 for the dimer $(PLY)_2$ (**Figure 6**), even though their behaviors have already been discussed in several previous studies[29,32].

Like the case of $(CH_3)_2$, y decreased monotonically with decreasing d_1, and $\gamma(N=2)$ showed a bell-shaped dependence on d_1. $\gamma(N = 2)$ attained a maximum around d_1 = 2.8 Å where y is in the intermediate region [at d_1 = 2.8 Å, $\gamma(N=2)$ = 7.3 x 10^4 a.u. and y_0 = 0.36].

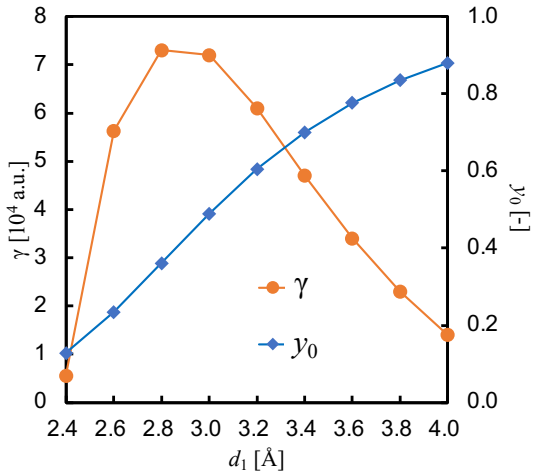

Figure 6. Stacking distance (d_1) dependences of y_0 and static $\gamma(N = 2)$ for the phenalenyl radical π-dimer calculated at the PUHF and LC-UBLYP(0.47) levels, respectively, using the 6-31G* basis set.

Then, we compared the results at the limit $N \rightarrow \infty$ for models with different d_1 and d_2 (**Figure 1b**). Calculations of γ for the N-mers of phenalenyls with large N, needed for estimating γ_∞, were time-consuming and numerically complex even with the DFT. Thus, we calculated γ_∞ directly based on the band structure calculations. In CRYSTAL 17, the fourth-order analytic derivative of total energy can be calculated based on the coupled-perturbed Kohn Sham (CPKS) method under the parodic boundary condition[35,43–45]. Salustro et al. evaluated the γ_∞ of 1D chains of phenalenyl radicals using the LC-UBLYP(0.33) functional using a development version of CRYSTAL[32]. They also proposed a rough estimation of γ_∞ at the UCCSD level by combining the results of the dimer at the UCCSD level with the polymer/dimer ratio [i.e., $\gamma_\infty/\gamma(N=2)$] estimated from the UHF and LC-UBLYP(0.33) calculations (15.0 ± 4.0). Here, we employed the LC-UBLYP(0.47) to calculate γ_∞. In the CRYSTAL 17 package, the single particle crystalline orbitals

are expressed as a linear combination of Bloch functions defined in terms of atomic orbital (AO) basis functions. We used the 6-31G* basis set without the diffuse function as the local AO basis. Salustro et al. employed a modified 6-31+(0.08)G* basis set (with a diffuse exponent of 0.08 upscaled from the original 0.04 value) to obtain the converged results of γ_∞ of the 1D chains of phenalenyl radicals[32]. Matsui et al. compared the LC-UBLYP(0.33) results with the 6-31+G* and 6-31G* basis sets for the 1D *N*-mer models of cyclic thiazyl radicals (DTDAs) with d = 3.1 Å and showed that the 6-31G* underestimated the 6-31+G* results less than 10%[31]. They also mentioned that the basis set superposition error (BSSE) effects on γ were negligible. We compared the LC-UBLYP(0.47) γ values for the dimer with different basis sets (**Figure S3**) and found that the 6-31G* is sufficient for our purpose. We also checked the parameter settings suitable for the band structure calculations using the CRYSTAL 17 package (see Supporting Information).

Figure 7 shows calculated $y_{av,\infty}$, $y_{SD,\infty}$, and γ_∞ for the infinite 1D chains as a function of d_1 with different SDA ratios d_2/d_1 (= 1.0, 1.2, and 2.0). We should note that Salustro et al. optimized geometries of the infinite 1D chains at the RB3LYP-D/6-31G* [(d_1, d_2) = (3.05Å, 3.19Å); d_2/d_1 ~ 1.05] and UB3LYP-D/6-31G* [(d_1, d_2) = (3.11Å, 3.12Å); d_2/d_1 ~ 1.00] levels. We here plotted the results in the range 2.8 Å ≤ d_1 ≤ 4.0 Å[32]. $y_{av,\infty}$ of these models were almost independent of the ratio d_2/d_1, whereas $y_{SD,\infty}$ for d_2/d_1 = 1.0 is about twice as large as that for d_2/d_1 = 1.2. $y_{SD,\infty}$ for d_2/d_1 = 2.0 were almost zero. γ_∞ enhanced significantly when d_1 is small and d_2/d_1 approached 1.0. These tendencies were similar to those obtained in the 1D chains of methyl radicals.

So far, there have been several reports of the synthesis of 1D stacked chains of phenalenyl radicals. For example, Uchida et al. reported the formation of the uniform 1D chains of 2,5,8-tris(pentafluorophenyl) phenalenyl radicals in the parallel stacking with d = 3.503 Å[22]. The distance is, however, larger than the vdW contact distance of the carbon atom (3.4 Å), and $y_{av,\infty}$ at d_1 = 3.5 Å, is estimated to be more than 0.7. Although d_2/d_1 = 1.0 was achieved, this 1D chain may not drastically enhance γ. Designing and synthesizing such uniform 1D chains requires tuning the balance between the attractive and repulsive interactions acting on each monomer and considering the entropic effects, which is challenging. However, from the stacking distances realized in the π-dimers of several derivatives of phenalenyl radicals, it may be possible to achieve the 1D chains with distances of about 3.1-3.2 Å[20]. If d_1 can be reduced to about 3.2 Å without the SDA, γ can be enhanced by about one order of magnitude compared with the dimer as a unit. Even if the SDA

patterns appear, we can still expect an enhancement of γ when the d_2/d_1 ratio is less than 1.2 [at d_1 = 3.2 Å, $\gamma_\infty/\gamma(N=2)$ = 9.5 for d_2/d_1 = 1.0 and $\gamma_\infty/\gamma(N=2)$ = 3.5 for d_2/d_1 = 1.2]. The obtained polymer/dimer ratio around d_1 = 3.2 Å is consistent with that predicted by Salustro et al. Regarding diradical characters, $y_{av,\infty} \leq 0.6$ and $y_{SD,\infty} \geq 0.1$ would be the target region for achieving severalfold enhancement of γ as a rough estimation from these results.

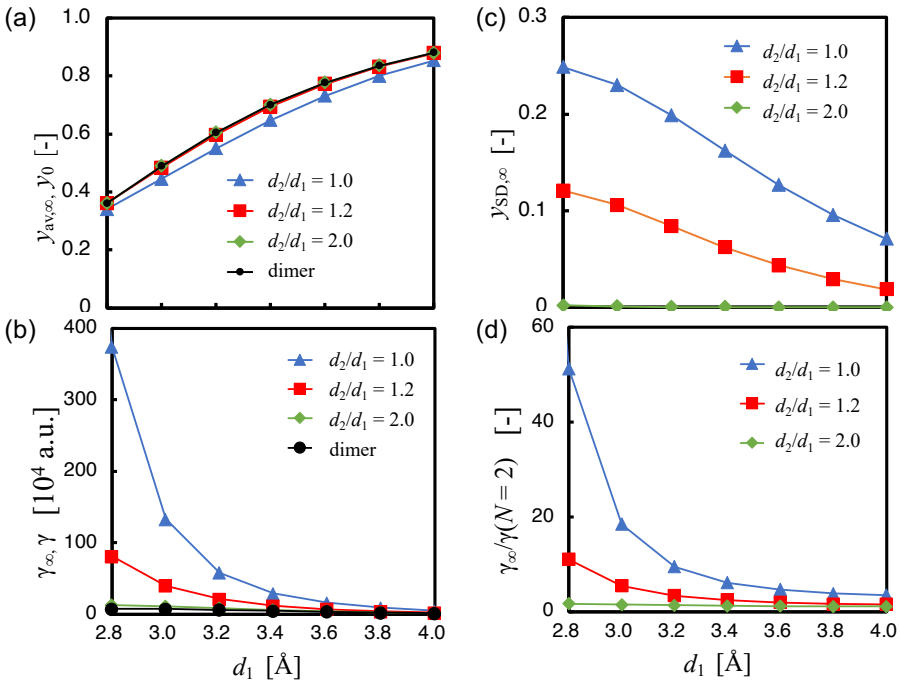

Figure 7. Stacking distance (d_1) dependences of (a) $y_{av,\infty}$, (b) $y_{SD,\infty}$, (c) γ_∞, and (d) $\gamma_\infty/\gamma(N=2)$ for the phenalenyl radical π-dimer calculated at the PUHF (for y) and LC-UBLYP(0.47) (for γ) levels, respectively, using the 6-31G* basis set.

On the other hand, although the present study focused on the dependence on the ratio of distances, the orbital interactions between the monomers tend to become smaller when the monomers are relatively slipped or rotated. We expect calculations and analysis based on y_{av} and y_{SD} to work for such cases. As an example, in **Figure 8**, we considered 1D chain models

introducing alternating misalignment (Δd_y) in the y-direction and calculated $y_{av,\infty}$, $y_{SD,\infty}$, and the polymer/dimer ratio $\gamma_\infty/\gamma(N = 2)$ with fixed $d_1 = 3.2$ Å and $d_2/d_1 = 1.0$. When we increased Δd_y, the orbital interactions between the monomers became weak, and as a result, $y_{av,\infty}$ increased while $y_{SD,\infty}$ decreased. In this case, $\gamma_\infty/\gamma(N = 2)$ was kept high when $y_{av,\infty} \leq 0.6$ and $y_{SD,\infty} \geq 0.1$. Thus, we expect that the combination of $y_{av,\infty}$ and $y_{SD,\infty}$ will help characterize the open-shell electronic structures in 1D chains with several different configurations.

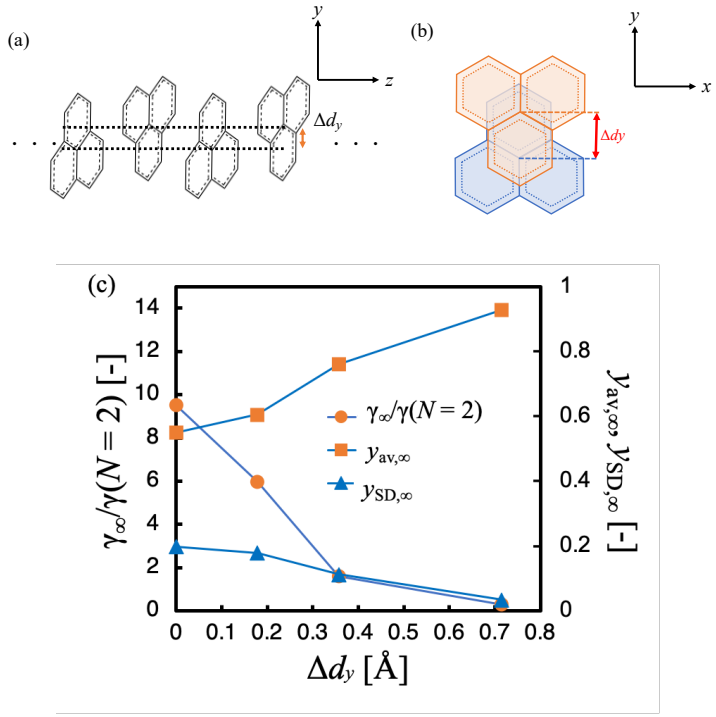

Figure 8. (a) Side and (b) top views of 1D chain models with alternating misalignment (Δd_y) in the y-direction and calculation results of $y_{av,\infty}$, $y_{SD,\infty}$, and (c) the polymer/dimer ratio $\gamma_\infty/\gamma(N = 2)$ with fixed $d_1 = 3.2$ Å and $d_2/d_1 = 1.0$.

4. CONCLUSIONS

In this paper, we theoretically investigated the correlation between open-shell electronic structure and third-order NLO properties of 1D chains of π-radicals. From the calculations of 1D

chain models consisting of methyl radicals, considering both the $y_{av,\infty}$ and $y_{SD,\infty}$ were important to characterize their open-shell electronic structures and discuss the γ_∞ values with the SDA. We also investigated the xc-functional dependence of γ_∞ and found that LC-UBLYP(0.47) reproduced well the γ_∞ values and their polymer/dimer ratio predicted at the UCCSD(T). By employing the LC-UBLYP(0.47) method, we also evaluated γ_∞ values of 1D chains of phenalenyl radicals. From the calculation results, 1D chains with $y_{av,\infty} \leq 0.6$ and $y_{SD,\infty} \geq 0.1$ are expected as candidates for novel third-order NLO materials with enhanced third-order NLO properties. These conditions can be met when the primary stacking distance is $d_1 \leq 3.2$ Å with a small SDA (d_2/d_1) ratio. The SDA and the relative configurations between the monomers affect the γ_∞ through the variation in y. Therefore, the combined use of $y_{av,\infty}$ and $y_{SD,\infty}$ will help clarify the relationship between open-shell electronic structures and third-order NLO properties in 1D chains of π-radicals.

On the other hand, to estimate $y_{av,\infty}$ and $y_{SD,\infty}$ at the PUHF level, one must prepare the initial guess carefully for large N and check the convergence behaviors of total energy and wavefunction to obtain physically meaningful calculation results. Alternatively, we suggest that one can roughly estimate the $y_{av,\infty}$ and $y_{SD,\infty}$ from the y_{av} and y_{SD} of $N = 4$ using eqs. (5)-(6) [see also the convergence behaviors of $y_{av}(N)$ and $y_{SD}(N)$ in **Figure 3**]. Of course, it must be beneficial if one can compute the $y_{av,\infty}$ and $y_{SD,\infty}$ (or their equivalents) from the quantum chemical calculations under the periodic boundary condition[46] consistent with the band gap and width results. We expect that utilizing the y-based indices introduced in this study also contributes to the further development of the data-driven exploration for novel open-shell functional materials [47].

In addition, the present results suggest that the enhanced third-order NLO properties can be expected for the 1D chains of phenalenyl radicals with $d_1 \leq 3.2$ Å while keeping SDA small. Exploration of appropriate substituent groups that assist stabilizing the uniform π-stacking

configuration in the crystal phase is highly desired. In this regard, it is necessary to comprehensively study the stabilization mechanism of the 1D chains with substituents, utilizing several analysis methods for intermolecular interactions, like those conducted for the dimers of phenalenyl radicals.[48–52]

Supporting Information.

The following files are available free of charge.

Comparison of calculation results at the UCCSD(T) and the LC-UBLYP with different range-separating parameters μ for 1D chains of methyl radicals, γ values at the UCCSD level for the 1D chain models of methyl radicals, parameter settings suitable for the CPKS analytic derivative calculations of 1D chains of phenalenyl radicals using CRYSTAL 17 program package, cartesian coordinate of the optimized geometries of the monomer unit (PDF)

AUTHOR INFORMATION

Corresponding Author

*Ryohei Kishi

Email: kishi.ryohei.es@osaka-u.ac.jp

Author Contributions

The manuscript was written through contributions of all authors. All authors have given approval to the final version of the manuscript.

Notes

The authors declare no competing financial interest.

ACKNOWLEDGMENT

This work is supported by JSPS KAKENHI Grant Nos. JP19H00912, JP21K04995, JP22H04974, JP22H02050, a Grant-in-Aid for Transformative Research Areas (A) "Condensed Conjugation" (Grant No. JP21H05489), and the International Collaborative Research Program of Institute for Chemical Research, Kyoto University (grant #2023-60 and #2024-53). W.Y. acknowledges financial support from the Center for Promotion of Advanced Interdisciplinary Research (Osaka Univ.) and the JSPS Fellowship (22KJ2166). R.S. acknowledges support from the Quantum LEAder Resource (QLEAR) fellowship program (Osaka University). Theoretical calculations were partly performed using Research Center for Computational Science, Okazaki, Japan (Project: 23-IMS-C004 and 24-IMS-C004).

REFERENCES

(1) *Nonlinear Optics of Organic Molecules and Polymers*, 1st Edition.; Nalwa, H. S., Miyata, S., Eds.; CRC Press: London, 1996.

(2) de Melo, C. P.; Silbey, R. Variational–Perturbational Treatment for the Polarizabilities of Conjugated Chains. I. Theory and Linear-polarizabilities Results for Polyenes. *J. Chem. Phys.* **1988**, *88* (4), 2558–2566. https://doi.org/10.1063/1.454035.

(3) Dawson, N. J.; Anderson, B. R.; Schei, J. L.; Kuzyk, M. G. Quantum Mechanical Model of the Upper Bounds of the Cascading Contribution to the Second Hyperpolarizability. *Phys. Rev. A* **2011**, *84* (4), 43407. https://doi.org/10.1103/PhysRevA.84.043407.

(4) Dawson, N. J.; Anderson, B. R.; Schei, J. L.; Kuzyk, M. G. Classical Model of the Upper Bounds of the Cascading Contribution to the Second Hyperpolarizability. *Phys. Rev. A* **2011**, *84* (4), 43406. https://doi.org/10.1103/PhysRevA.84.043406.

(5) Tykwinski, R. R.; Gubler, U.; Martin, R. E.; Diederich, F.; Bosshard, C.; Günter, P. Structure−Property Relationships in Third-Order Nonlinear Optical Chromophores. *J. Phys. Chem. B* **1998**, *102* (23), 4451–4465. https://doi.org/10.1021/jp980829o.

(6) Meyers, F.; Marder, S. R.; Pierce, B. M.; Bredas, J. L. Electric Field Modulated Nonlinear Optical Properties of Donor-Acceptor Polyenes: Sum-Over-States Investigation of the Relationship between Molecular Polarizabilities (α, β, and γ) and Bond Length Alternation. *J. Am. Chem. Soc.* **1994**, *116* (23), 10703–10714. https://doi.org/10.1021/ja00102a040.

(7) Karna, S. P.; Talapatra, G. B.; Wijekoon, W. M. K. P.; Prasad, P. N. Frequency Dependence of Linear and Nonlinear Optical Properties of Conjugated Polyenes: An Ab Initio Time-Dependent Coupled Hartree-Fock Study. *Phys. Rev. A* **1992**, *45* (5), 2763–2770. https://doi.org/10.1103/PhysRevA.45.2763.

(8) Heflin, J. R.; Wong, K. Y.; Zamani-Khamiri, O.; Garito, A. F. Nonlinear Optical Properties of Linear Chains and Electron-Correlation Effects. *Phys. Rev. B* **1988**, *38* (2), 1573–1576. https://doi.org/10.1103/PhysRevB.38.1573.

(9) Nakano, M.; Champagne, B. Nonlinear Optical Properties in Open-Shell Molecular Systems. *WIREs Computational Molecular Science* **2016**, *6* (2), 198–210. https://doi.org/https://doi.org/10.1002/wcms.1242.

(10) Matsui, H.; Nakano, M.; Champagne, B. Theoretical Study on the Spin State and Open-Shell Character Dependences of the Second Hyperpolarizability in Hydrogen Chain Models. *Phys. Rev. A* **2016**, *94* (4), 42515. https://doi.org/10.1103/PhysRevA.94.042515.

(11) Nakano, M. Open-Shell-Character-Based Molecular Design Principles: Applications to Nonlinear Optics and Singlet Fission. *Chemical Record* **2017**, *17* (1), 27–62. https://doi.org/10.1002/tcr.201600094.

(12) Matsui, H.; Ito, S.; Nakano, M. Open-Shell Character Dependences of the Second Hyperpolarizability in Two-Dimensional Tetraradicaloids. *J. Phys. Chem. A* **2018**, *122* (14), 3680–3687. https://doi.org/10.1021/acs.jpca.7b12456.

(13) Nakano, M.; Kishi, R.; Ohta, S.; Takahashi, H.; Kubo, T.; Kamada, K.; Ohta, K.; Botek, E.; Champagne, B. Relationship between Third-Order Nonlinear Optical Properties and Magnetic Interactions in Open-Shell Systems: A New Paradigm for Nonlinear Optics. *Phys. Rev. Lett.* **2007**, *99* (3), 033001. https://doi.org/10.1103/PhysRevLett.99.033001.

(14) Nakano, M.; Nagao, H.; Yamaguchi, K. Many-Electron Hyperpolarizability Density Analysis: Application to the Dissociation Process of One-Dimensional H_2. *Phys. Rev. A.* **1997**, *55* (2), 1503–1513. https://doi.org/10.1103/PhysRevA.55.1503.

(15) *Diradicaloids*, 1st Edition.; Wu, J., Ed.; Jenny Stanford Publishing: New York, 2022.

(16) Hinz, A.; Bresien, J.; Breher, F.; Schulz, A. Heteroatom-Based Diradical(oid)s. *Chem. Rev.* **2023**, *123* (16), 10468–10526. https://doi.org/10.1021/acs.chemrev.3c00255.

(17) Shu, C.; Yang, Z.; Rajca, A. From Stable Radicals to Thermally Robust High-Spin Diradicals and Triradicals. *Chem. Rev.* **2023**, *123* (20), 11954–12003. https://doi.org/10.1021/acs.chemrev.3c00406.

(18) Ishigaki, Y.; Harimoto, T.; Shimajiri, T.; Suzuki, T. Carbon-Based Biradicals: Structural and Magnetic Switching. *Chem. Rev.* **2023**, *123* (24), 13952–13965. https://doi.org/10.1021/acs.chemrev.3c00376.

(19) Abe, M. Diradicals. *Chem. Rev.* **2013**, *113* (9), 7011–7088. https://doi.org/10.1021/cr400056a.

(20) Kertesz, M. Pancake Bonding: An Unusual Pi-Stacking Interaction. *Chem. Eur. J.* **2019**, *25* (2), 400–416. https://doi.org/https://doi.org/10.1002/chem.201802385.

(21) Kubo, T.; Shimizu, A.; Sakamoto, M.; Uruichi, M.; Yakushi, K.; Nakano, M.; Shiomi, D.; Sato, K.; Takui, T.; Morita, Y. et al. Synthesis, Intermolecular Interaction, and Semiconductive Behavior of a Delocalized Singlet Biradical Hydrocarbon. *Angew. Chem. Int. Ed.* **2005**, *44* (40), 6564–6568. https://doi.org/https://doi.org/10.1002/anie.200502303.

(22) Uchida, K.; Hirao, Y.; Kurata, H.; Kubo, T.; Hatano, S.; Inoue, K. Dual Association Modes of the 2,5,8-Tris(Pentafluorophenyl)Phenalenyl Radical. *Chem. Asian J.* **2014**, *9* (7), 1823–1829. https://doi.org/https://doi.org/10.1002/asia.201402187.

(23) Koutentis, P. A.; Chen, Y.; Cao, Y.; Best, T. P.; Itkis, M. E.; Beer, L.; Oakley, R. T.; Cordes, A. W.; Brock, C. P.; Haddon, R. C. Perchlorophenalenyl Radical. *J. Am. Chem. Soc.* **2001**, *123* (17), 3864–3871. https://doi.org/10.1021/ja0018015.

(24) Bryan, C. D.; Cordes, A. W.; Haddon, R. C.; Hicks, R. G.; Kennepohl, D. K.; MacKinnon, C. D.; Oakley, R. T.; Palstra, T. T. M.; Perel, A. S.; al.., et. Molecular Conductors from Neutral-Radical Charge-Transfer Salts: Preparation and Characterization of an I Doped Hexagonal Phase of 1,2,3,5-Dithiadiazolyl ([HCN2S2].Bul.). *J. Am. Chem. Soc.* **1994**, *116* (4), 1205–1210. https://doi.org/10.1021/ja00083a005.

(25) Suizu, R.; Iwasaki, A.; Shuku, Y.; Awaga, K. Spatially Inhomogeneous, Stepwise Phase Transitions in a Thiazyl Diradical: A Structural Mismatch Induced by Lattice Transformation. *J. Mater. Chem. C* **2015**, *3* (30), 7968–7977. https://doi.org/10.1039/C5TC01410G.

(26) Cordes, A. W.; Bryan, C. D.; Davis, W. M.; de Laat, R. H.; Glarum, S. H.; Goddard, J. D.; Haddon, R. C.; Hicks, R. G.; Kennepohl, D. K. Prototypal 1,2,3,5-Dithia- and -Diselenadiazolyl [HCN2E2].Bul. (E = Sulfur, Selenium): Molecular and Electronic Structures of the Radicals and Their Dimers, by Theory and Experiment. *J. Am. Chem. Soc.* **1993**, *115* (16), 7232–7239. https://doi.org/10.1021/ja00069a022.

(27) Vela, S.; Mota, F.; Deumal, M.; Suizu, R.; Shuku, Y.; Mizuno, A.; Awaga, K.; Shiga, M.; Novoa, J. J.; Ribas-Arino, J. The Key Role of Vibrational Entropy in the Phase Transitions of Dithiazolyl-Based Bistable Magnetic Materials. *Nat. Commun.* **2014**, *5* (1), 4411. https://doi.org/10.1038/ncomms5411.

(28) Beneberu, H. Z.; Tian, Y.-H.; Kertesz, M. Bonds or Not Bonds? Pancake Bonding in 1,2,3,5-Dithiadiazolyl and 1,2,3,5-Diselenadiazolyl Radical Dimers and Their Derivatives. *Phys. Chem. Chem. Phys.* **2012**, *14* (30), 10713–10725. https://doi.org/10.1039/C2CP41018D.

(29) Yoneda, K.; Nakano, M.; Fukuda, K.; Matsui, H.; Takamuku, S.; Hirosaki, Y.; Kubo, T.; Kamada, K.; Champagne, B. Third-Order Nonlinear Optical Properties of One-Dimensional Open-Shell Molecular Aggregates Composed of Phenalenyl Radicals. *Chem. Eur. J.* **2014**, *20* (35), 11129–11136. https://doi.org/https://doi.org/10.1002/chem.201402197.

(30) Matsui, H.; Yamane, M.; Tonami, T.; Nagami, T.; Watanabe, K.; Kishi, R.; Kitagawa, Y.; Nakano, M. Theoretical Study on the Gigantic Effect of External Static Electric Field Application on the Nonlinear Optical Properties of 1,2,3,5-Dithiadiazolyl π-Radical Dimers. *Mater. Chem. Front.* **2018**, *2* (4), 785–790. https://doi.org/10.1039/c7qm00549k.

(31) Matsui, H.; Yamane, M.; Tonami, T.; Nakano, M.; de Wergifosse, M.; Seidler, T.; Champagne, B. Theoretical Study on Third-Order Nonlinear Optical Property of One-Dimensional Cyclic Thiazyl Radical Aggregates: Intermolecular Distance, Open-Shell Nature, and Spin State Dependences. *J. Phys. Chem. C* **2018**, *122* (12), 6779–6785. https://doi.org/10.1021/acs.jpcc.7b11319.

(32) Salustro, S.; Maschio, L.; Kirtman, B.; Rérat, M.; Dovesi, R. Third-Order Electric Field Response of Infinite Linear Chains Composed of Phenalenyl Radicals. *J. Phys. Chem. C* **2016**, *120* (12), 6756–6761. https://doi.org/10.1021/acs.jpcc.6b01077.

(33) Nakano, M.; Takebe, A.; Kishi, R.; Ohta, S.; Nate, M.; Kubo, T.; Kamada, K.; Ohta, K.; Champagne, B.; Botek, E. et al. Second Hyperpolarizabilities (γ) of Open-Shell Singlet One-Dimensional Systems: Intersite Interaction Effects on the Average Diradical Character and Size Dependences of γ. *Chem. Phys. Lett.* **2006**, *432* (4–6), 473–479. https://doi.org/10.1016/j.cplett.2006.10.082.

(34) Dovesi, R.; Orlando, R.; Erba, A.; Zicovich-Wilson, C. M.; Civalleri, B.; Casassa, S.; Maschio, L.; Ferrabone, M.; De La Pierre, M.; D'Arco, P. et al. CRYSTAL14: A Program for the Ab Initio Investigation of Crystalline Solids. *Int. J. Quantum Chem.* **2014**, *114* (19), 1287–1317. https://doi.org/https://doi.org/10.1002/qua.24658.

(35) Dovesi, R.; Erba, A.; Orlando, R.; Zicovich-Wilson, C. M.; Civalleri, B.; Maschio, L.; Rérat, M.; Casassa, S.; Baima, J.; Salustro, S.; Kirtman, B. Quantum-Mechanical Condensed Matter Simulations with CRYSTAL. *WIREs Computational Molecular Science* **2018**, *8* (4), e1360. https://doi.org/https://doi.org/10.1002/wcms.1360.

(36) Yoshida, W.; Matsui, H.; Miyamoto, H.; Tonami, T.; Sugimori, R.; Yoneda, K.; Kishi, R.; Nakano, M. Theoretical Study on Third-Order Nonlinear Optical Properties for One-Hole-Doped Diradicaloids. *ACS Omega* **2021**, *6* (4), 3046–3059. https://doi.org/10.1021/acsomega.0c05424.

(37) Yamaguchi, K. The Electronic Structures of Biradicals in the Unrestricted Hartree-Fock Approximation. *Chem. Phys. Lett.* **1975**, *33* (2), 330–335. https://doi.org/10.1016/0009-2614(75)80169-2.

(38) Tawada, Y.; Tsuneda, T.; Yanagisawa, S.; Yanai, T.; Hirao, K. A Long-Range-Corrected Time-Dependent Density Functional Theory. *J. Chem. Phys.* **2004**, *120* (18), 8425–8433. https://doi.org/10.1063/1.1688752.

(39) Iikura, H.; Tsuneda, T.; Yanai, T.; Hirao, K. A Long-Range Correction Scheme for Generalized-Gradient-Approximation Exchange Functionals. *J. Chem. Phys.* **2001**, *115* (8), 3540–3544. https://doi.org/10.1063/1.1383587.

(40) Kishi, R.; Bonness, S.; Yoneda, K.; Takahashi, H.; Nakano, M.; Botek, E.; Champagne, B.; Kubo, T.; Kamada, K.; Ohta, K.; Tsuneda, T. Long-Range Corrected Density Functional Theory Study on Static Second Hyperpolarizabilities of Singlet Diradical Systems. *J. Chem. Phys.* **2010**, *132* (9), 094107. https://doi.org/10.1063/1.3332707.

(41) Frisch, M. J.; Trucks, G. W.; Schlegel, H. B.; Scuseria, G. E.; Robb, M. A.; Cheeseman, J. R.; Scalmani, G.; Barone, V.; Mennucci, B.; Petersson, G. A. et al. Gaussian09 Revision D.01.

(42) Nakano, M.; Shigemoto, I.; Yamada, S.; Yamaguchi, K. Size-consistent Approach and Density Analysis of Hyperpolarizability: Second Hyperpolarizabilities of Polymeric Systems with and without Defects. *J. Chem. Phys.* **1995**, *103* (10), 4175–4191. https://doi.org/10.1063/1.470657.

(43) Orlando, R.; Lacivita, V.; Bast, R.; Ruud, K. Calculation of the First Static Hyperpolarizability Tensor of Three-Dimensional Periodic Compounds with a Local Basis Set: A Comparison of LDA, PBE, PBE0, B3LYP, and HF Results. *J. Chem. Phys.* **2010**, *132* (24), 244106. https://doi.org/10.1063/1.3447387.

(44) Ferrero, M.; Civalleri, B.; Rérat, M.; Orlando, R.; Dovesi, R. The Calculation of the Static First and Second Susceptibilities of Crystalline Urea: A Comparison of Hartree–Fock and Density Functional Theory Results Obtained with the Periodic Coupled Perturbed Hartree–Fock/Kohn–Sham Scheme. *J. Chem. Phys.* **2009**, *131* (21), 214704. https://doi.org/10.1063/1.3267861.

(45) Orlando, R.; Bast, R.; Ruud, K.; Ekström, U.; Ferrabone, M.; Kirtman, B.; Dovesi, R. The First and Second Static Electronic Hyperpolarizabilities of Zigzag Boron Nitride Nanotubes. An Ab Initio Approach through the Coupled Perturbed Kohn–Sham Scheme. *J. Phys. Chem. A* **2011**, *115* (45), 12631–12637. https://doi.org/10.1021/jp203237m.

(46) Tada, K.; Kitagawa, Y.; Kawakami, T.; Okumura, M.; Tanaka, S. Electron Density-Based Estimation of Diradical Character: An Easy Scheme for DFT/Plane-Wave Calculations. *Chem. Lett.* **2021**, *50* (2), 392–396. https://doi.org/10.1246/cl.200741.

(47) Hayashi, Y.; Kawauchi, S. Development of a Quantum Chemical Descriptor Expressing Aromatic/Quinoidal Character for Designing Narrow-Bandgap π-Conjugated Polymers. *Polym. Chem.* **2019**, *10* (41), 5584–5593. https://doi.org/10.1039/C9PY00987F.

(48) Takano, Y.; Taniguchi, T.; Isobe, H.; Kubo, T.; Morita, Y.; Yamamoto, K.; Nakasuji, K.; Takui, T.; Yamaguchi, K. Effective Exchange Integrals and Chemical Indices for a Phenalenyl Radical Dimeric Pair. *Chem. Phys. Lett.* **2002**, *358* (1), 17–23. https://doi.org/https://doi.org/10.1016/S0009-2614(02)00537-7.

(49) Zaitsev, V.; Rosokha, S. V; Head-Gordon, M.; Kochi, J. K. Steric Modulations in the Reversible Dimerizations of Phenalenyl Radicals via Unusually Weak Carbon-Centered π- and σ-Bonds. *J. Org. Chem.* **2006**, *71* (2), 520–526. https://doi.org/10.1021/jo051612a.

(50) Cui, Z.; Lischka, H.; Beneberu, H. Z.; Kertesz, M. Rotational Barrier in Phenalenyl Neutral Radical Dimer: Separating Pancake and van Der Waals Interactions. *J. Am. Chem. Soc.* **2014**, *136* (15), 5539–5542. https://doi.org/10.1021/ja412862n.

(51) Tang, Z.; Jiang, Z.; Chen, H.; Su, P.; Wu, W. Energy Decomposition Analysis Based on Broken Symmetry Unrestricted Density Functional Theory. *J. Chem. Phys.* **2019**, *151* (24), 244106. https://doi.org/10.1063/1.5114611.

(52) Cui, Z.; Wang, M.; Lischka, H.; Kertesz, M. Unexpected Charge Effects Strengthen π–Stacking Pancake Bonding. *JACS Au* **2021**, *1* (10), 1647–1655. https://doi.org/10.1021/jacsau.1c00272.

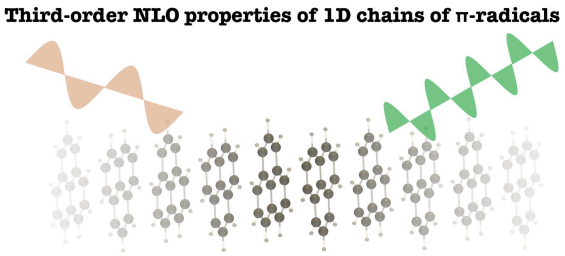

TOC Graphic